












RESEARCH ARTICLE | MAY 20 2024

## Self-aligned formation of superconducting sub-5 nm PtSi films

Yao Yao ; Daniel F. Fernandes ; Tereza Košutová ; Tomas Kubart ; Zhen Zhang ;  
François Lefloch ; Frédéric Gustavo; Axel Leblanc ; János L. Lábár ; Béla Pécz ; Shi-Li Zhang  



APL Quantum 1, 026112 (2024)

<https://doi.org/10.1063/5.0205444>



View  
Online



Export  
Citation



## APL Quantum

### First Articles Online

No Article Processing Charges for Submissions  
Through December 31, 2024

**Read Now**

# Self-aligned formation of superconducting sub-5 nm PtSi films

Cite as: APL Quantum 1, 026112 (2024); doi: 10.1063/5.0205444

Submitted: 26 February 2024 • Accepted: 6 May 2024 •

Published Online: 20 May 2024



Yao Yao,<sup>1</sup> Daniel F. Fernandes,<sup>1</sup> Tereza Košutová,<sup>1</sup> Tomas Kubart,<sup>1</sup> Zhen Zhang,<sup>1</sup> François Lefloch,<sup>2</sup> Frédéric Gustavo,<sup>2</sup> Axel Leblanc,<sup>2</sup> János L. Lábár,<sup>3</sup> Béla Pécz,<sup>3</sup> and Shi-Li Zhang<sup>1,a)</sup>

## AFFILIATIONS

<sup>1</sup> Division of Solid-State Electronics, Department of Electrical Engineering, Uppsala University, Uppsala 751 03, Sweden

<sup>2</sup> Université Grenoble Alpes, CEA, Grenoble INP, IRIG, PHELIQS, 38000 Grenoble, France

<sup>3</sup> Thin Film Physics Laboratory, Institute of Technical Physics and Materials Science, HUN-REN Centre for Energy Research, H-1121 Budapest, Hungary

<sup>a)</sup> Author to whom correspondence should be addressed: [Shili.Zhang@angstrom.uu.se](mailto:Shili.Zhang@angstrom.uu.se)

## ABSTRACT

Platinum silicide (PtSi) presents a promising superconductor for achieving silicon-based Josephson field-effect transistors (JoFETs). In a viable process flow to realize self-aligned PtSi formation, thermal oxidation at 600 °C is required to form a protective oxide layer on the surface of the as-formed PtSi selectively against Pt to facilitate subsequent selective etch in aqua regia. However, sub-10 nm PtSi films tend to agglomerate and even break into discrete PtSi islands upon thermal treatments above 500 °C. To achieve nanoscale JoFETs, we have developed a simple alternative with chemical oxidation at room temperature leading to the formation of homogeneous sub-5 nm PtSi films. The critical temperature of the resultant superconducting PtSi films is found to increase from 0.66 to 0.90 K when the PtSi thickness is raised from 3.1 to 12.7 nm, while, concurrently, the PtSi grains grow larger in thicker films. The critical temperature also increases from 0.53 to 0.66 K for the 3.1 nm PtSi film when the formation temperature is raised from 400 to 500 °C.

© 2024 Author(s). All article content, except where otherwise noted, is licensed under a Creative Commons Attribution-NonCommercial 4.0 International (CC BY-NC) license (<https://creativecommons.org/licenses/by-nc/4.0/>). <https://doi.org/10.1063/5.0205444>

Quantum computing holds promises in solving outstanding problems that are difficult for conventional computers to tackle.<sup>1</sup> An example is drug development involving complex molecular interactions among thousands of molecules.<sup>2</sup> The demand of large-scale quantum computing for such computational tasks motivates research on semiconducting quantum bits whose fabrication is compatible with advanced complementary metal-oxide semiconductor (CMOS) technology.<sup>3</sup> In this respect, silicon-based Josephson field-effect transistors (JoFETs) with superconducting source and drain terminals are considered as possible gate-tunable Josephson junctions to support a scalable alternative to superconducting quantum bits based on the Josephson tunnel junction. In possession of a relatively low Schottky barrier height to holes, platinum silicide (PtSi) as one of the CMOS-compatible metallization materials,<sup>4</sup> presents a promising superconductor in a JoFET that is essentially a Schottky barrier source/drain FET. The superconductivity of PtSi films has been studied and applied in Josephson junctions,<sup>5</sup> electron cooling,<sup>6</sup> and photon sensors.<sup>7</sup> Recently, PtSi

has been investigated as the metallic source and drain contact of Schottky-barrier metal-oxide-semiconductor field-effect transistors in cryogenic CMOS and in the context of quantum superconducting technology based on nanoscale JoFETs.<sup>8</sup> To support the development of nanoscale JoFETs that would ultimately be manufactured along with the control and readout electronics on the same substrate wafer,<sup>9</sup> a CMOS-compatible process flow is essential for the formation of ultrathin superconducting PtSi films below 5 nm in thickness yet retaining high morphological integrity and attaining the critical temperature ( $T_C$ ) of bulk PtSi.

The formation of a PtSi film usually starts from physical vapor deposition on a precleaned silicon substrate of a platinum layer with a thickness of about half that of the target PtSi film.<sup>10</sup> It is followed by rapid thermal processing (RTP) typically ranging from 350 to 600 °C.<sup>6,11–16</sup> At the low temperature limit, metal-rich nonsuperconducting Pt<sub>2</sub>Si can stay untransformed to PtSi if the annealing temperature is below 400 °C.<sup>11,16–18</sup> For PtSi films below 10 nm in thickness, agglomeration, which can degrade the electrical con-

ductivity causing contact failure, may occur already at annealing temperatures below 600 °C.<sup>19,20</sup> A successful self-aligned PtSi process requires a selective removal of unreacted Pt with the formed PtSi being protected by a surface oxide layer against the etchant aqua regia.<sup>14,21</sup> To alleviate the adverse effects of oxygen on the PtSi formation,<sup>22</sup> a two-step process was demonstrated, the formation of PtSi at 500 °C in a nitrogen atmosphere and, immediately after, the growth of an ultrathin SiO<sub>2</sub> layer on PtSi (but not on Pt) by means of thermal oxidation at 600 °C in an oxygen atmosphere.<sup>21</sup> Oxidation temperature lower than 600 °C was proven insufficient to form a quality protective SiO<sub>2</sub> layer against aqua regia attack of PtSi. Concurrently, surface treatment of PtSi in piranha (a mixed solution of H<sub>2</sub>SO<sub>4</sub> and H<sub>2</sub>O<sub>2</sub>) below 100 °C has been reported to produce a continuous PtSi<sub>2</sub>O<sub>4</sub> cap layer.<sup>23</sup>

In this work, the chemical oxidation of PtSi in piranha is investigated as a low-temperature route for surface protection of ultrathin PtSi films during the subsequent selective etch in aqua regia. The robustness and scalability of the process flow are confirmed by the successful formation of ultrathin PtSi films below 5 nm, thereby presenting a simple and reliable self-aligned PtSi process. In addition to various room-temperature (RT) characterizations,  $T_C$  of the superconducting PtSi films is found to be higher than previously reported data. This study extends to the effect of annealing temperature on  $T_C$  of superconducting PtSi thin films.

Silicon-on-insulator wafers, 300 mm in diameter with an ultrathin *p*-type surface Si layer of 16 nm in thickness and resistivity of 10–15 Ω cm, were used in this work. Immediately prior to each metal deposition, standard wafer cleaning ended by removing the grown chemical oxide in a dilute HF solution (1%). Platinum films with nominal thickness of 1.5–7.5 nm were deposited by means of magnetron sputtering without substrate heating, using a Pt target of 99.99% purity in an ultrahigh vacuum sputter-deposition system. The self-aligned silicide (SALICIDE) process was conducted for all samples with the aforementioned RTP step in a N<sub>2</sub> atmosphere at different temperatures all for 30 s. Two different methods for surface oxidation were evaluated: (1) thermal oxidation (Therm-ox) at 600 °C for 1 min in the same RTP chamber as done before<sup>21</sup> and (2) chemical oxidation (Chem-ox) in piranha below 100 °C. Selective wet etch of Pt in diluted aqua regia (H<sub>2</sub>O:HCl:HNO<sub>3</sub> = 4:3:1) at 85 °C for 2 min was carried out after surface oxidation. For thin-film studies at RT, Rutherford backscattering spectrometry (RBS) was employed for Pt thickness calibration; grazing incidence x-ray diffraction (GIXRD) for confirmation of PtSi formation and estimation of PtSi grain size according to Scherrer equation<sup>24</sup> using the diffraction peak of {110} planes and by employing the whole-powder pattern fitting<sup>25</sup> for selected samples; sheet resistance ( $R_S$ ) measurement using a four-point probe setup in combination with the RBS and GIXRD data for determination of the resistivity of PtSi films formed in the temperature range used; and scanning electron microscope (SEM), transmission electron microscopy (TEM), and energy dispersive spectroscopy (EDS) for morphology inspection and atomic composition analysis. The superconducting properties of PtSi thin films were studied by performing resistance measurements at very low temperatures. The resistance of the various samples was measured using lock-in techniques with low-noise amplifiers at low frequencies (typically below 100 Hz). An optimum low AC current (less than 1 μA) was applied to avoid heating in the resistive state. The superconducting transition temperature (*i.e.*,  $T_C$ ) was

obtained using two different cryogenics systems for reproducibility check.

The resulting PtSi thickness,  $d_{\text{PtSi}}$ , of the samples from 3.1 to 12.7 nm represents the product of the RBS Pt thickness and the volumetric expansion factor for converting Pt to PtSi.<sup>10</sup> The dependence of RT PtSi resistivity ( $\rho$ , the product of sheet resistance and film thickness) on  $d_{\text{PtSi}}$  is shown in Fig. 1(a), while the variation of  $T_C$  with  $d_{\text{PtSi}}$  is shown in Fig. 1(b) for PtSi films formed under different conditions of temperature and atmosphere along with published data in the literature.<sup>6,12,15</sup> Several observations can be made. First, the annealing temperature is found to have negligible effects on  $\rho$  at each given  $d_{\text{PtSi}}$ . Second,  $T_C$  approaching that of bulk PtSi (about 1 K<sup>6</sup>) is achieved in our study. Third, thicker PtSi films are characterized by higher  $T_C$  in agreement with the previously reported results.<sup>6,12,15</sup> Fourth, the general observation is  $T_C$  increasing with the formation temperature for the PtSi films of the same  $d_{\text{PtSi}}$  among the data points shown in Fig. 1(b). Thickness dependence of  $T_C$  is usually observed for thin films. The origin is most likely due to the change in the Fermi velocity or electron mean free path that directly affects the superconducting gap and, therefore  $T_C$ ,<sup>26,27</sup> which is consistent with the observation of decrease in  $T_C$  with increasing RT  $R_S$ , as shown in Fig. 1(c). Variations in  $T_C$  for the samples with the lower annealing temperatures [Figs. 1(b) and 1(c)] have also been observed for other superconducting materials.<sup>28</sup> By applying the universal scaling law<sup>28</sup> to our films, *i.e.*, plotting  $d_{\text{PtSi}} \cdot T_C$  as a function of RT  $R_S$ , as shown in Fig. 1(d), all the data points follow the same trend that can be excellently described by a simple relationship,  $d_{\text{PtSi}} \cdot T_C = A \cdot R_S^{-B}$ , with  $A = 273$  and  $B = 0.9$ . The value of the  $B$  exponent is close to those for NbN and other superconducting films.<sup>28</sup> The agreement between the experiment and model also confirms that our growth system is stable. Fluctuations in the film thickness were observed in the samples annealed at 400 °C by cross-sectional TEM (XTEM). Higher formation temperature induces a faster conversion of Pt to PtSi and lower probability of retaining the precursor nonsuperconducting Pt-rich silicide phases.<sup>11</sup> Thus, 500 °C was applied as the formation temperature of ultrathin superconducting PtSi films for further investigations.

The effect of Therm-ox at 600 °C on the integrity of the PtSi films formed at 500 °C can be inferred by examining the variation of RT  $R_S$  along with the average PtSi grain size with annealing temperature shown in Fig. 2(a). The samples underwent the entire process intended for SALICIDE: annealing for PtSi formation, surface oxidation of PtSi, and selective etch of Pt in aqua regia. As a reference, the variation of RT  $R_S$  for the as-annealed PtSi films prior to the Therm-ox step is shown in Fig. 2(a). The estimated grain size from the (110) peak that corresponds to the dimension almost perpendicular to the sample surface coincides well with the  $d_{\text{PtSi}}$ . The whole-powder pattern fitting further shows that the dimension of crystalline grains does not vary significantly with the inclination to the surface. The increase in lateral average grain size with  $d_{\text{PtSi}}$  is also observed for thicker PtSi films.<sup>19</sup> A positive correlation between  $T_C$  and the (lateral) PtSi grain size is, therefore, confirmed, as also seen in other silicides, such as V<sub>3</sub>Si.<sup>29</sup> Further measurements of the grain size for the samples already shown in Fig. 1(a) suggest that the grain size is not sensitive to the formation temperature for PtSi films of the same initial Pt thickness, which is also the case for  $\rho$  shown in Fig. 1(a). For the case of the thinnest PtSi film (3.1 nm thick), a con-

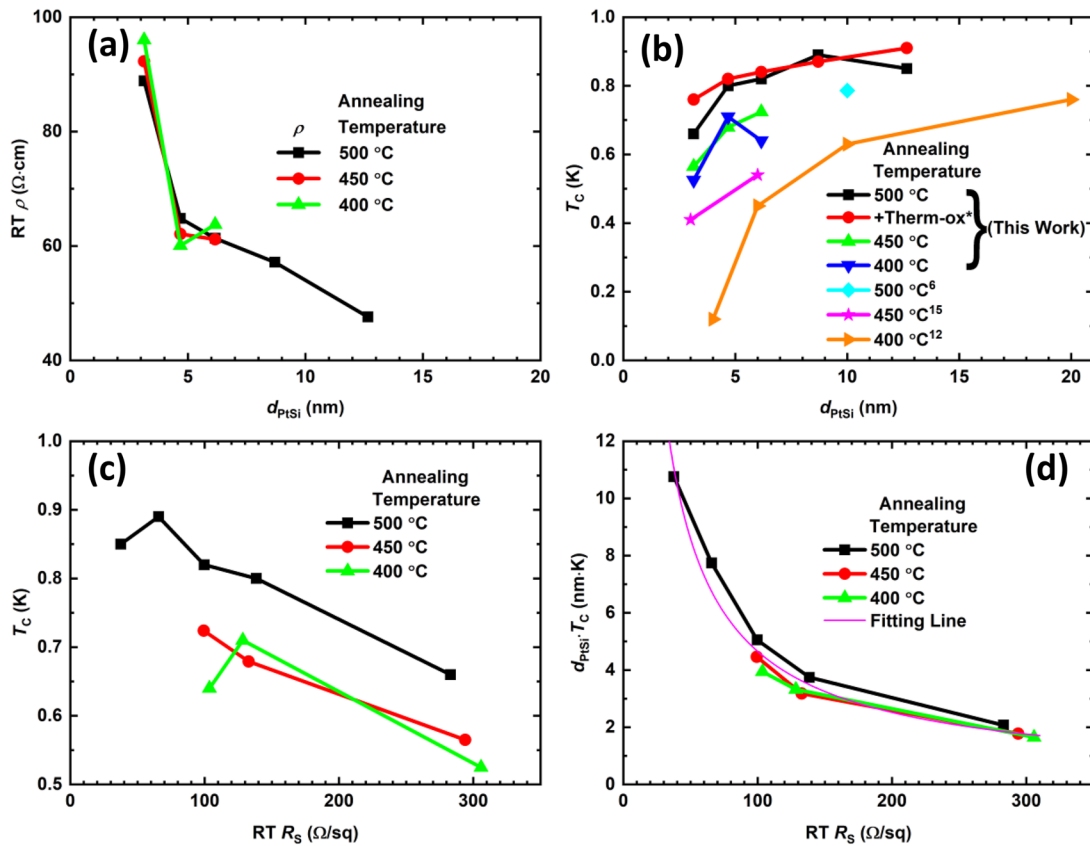


**FIG. 1.** (a) Room-temperature resistivity,  $RT \rho$ , as a function of PtSi thickness,  $d_{\text{PtSi}}$ , for PtSi films formed at different temperatures. (b) Critical temperature,  $T_C$ , as a function of  $d_{\text{PtSi}}$  for PtSi films formed at different temperatures in comparison with the literature data. The highest  $T_C$  is close to that of bulk PtSi (about 1 K<sup>6</sup>). \*: annealing at 500 °C, followed by thermal oxidation at 600 °C. (c)  $T_C$ , as a function of room-temperature sheet resistance,  $RT R_s$ , for PtSi films formed at different temperatures. (d)  $d_{\text{PtSi}} \cdot T_C$  as a function of  $RT R_s$ , for PtSi films formed at different temperatures with its fit to the universal scaling law for thin films ( $d_{\text{PtSi}} \cdot T_C = A \cdot R_s^{-B}$ ).<sup>28</sup>  $A = 273$  and  $B = 0.9$ .

tinuous and homogeneous layer is seen for the as-annealed sample shown in Fig. 2(b). The sample suffers from a threefold increase in  $RT R_s$  upon Therm-ox, compared to the as-annealed sample, which is obviously a consequence of agglomeration of the PtSi film shown in Fig. 2(c). The agglomeration is mainly caused by the thermal effect, and oxidation appears to play a minor role because the fraction of exposed Si for the sample with oxidation shown in Fig. 2(c) (50%) is close to that for the control sample shown in Fig. 2(d) (48%), which underwent the same thermal process but without oxidation (*i.e.*, annealed first at 500 °C for 30 s and then at 600 °C for 1 min, both in  $N_2$ ). This seemingly minor morphological improvement is accompanied by an appreciable decrease in  $RT R_s$  [the blue star shown in Fig. 2(a)] from that of the Therm-ox sample. The homogeneous PtSi in the as-annealed sample [Fig. 2(b)] and the agglomerated PtSi in the Therm-ox sample [Fig. 2(c)] are well visible in the XTEM micrographs shown in Figs. 2(e) and 2(f), respectively.

The flatness of the surface despite the severe agglomeration of PtSi film shown in Fig. 2(f) is dictated by the minimization of surface energy for the invariant volume and thus free energy of PtSi (thermodynamics) and attained due to the highly mobile Pt and

Si atoms in PtSi<sup>30</sup> (kinetics). Apparently, the contrast shown in Figs. 2(c) and 2(d) is primarily material not height-caused. Agglomeration was also observed in the 4.7–12.7 nm PtSi films after the Therm-ox, but to a much lesser extent with a quickly decreasing fraction of exposed Si with increasing PtSi thickness (*i.e.*, 21% for the 4.7 nm thick PtSi film). Such a degradation in PtSi films negatively affects the electrical performance and reliability. Moreover, the  $T_C$  of the 3.1 nm thick PtSi film in the as-annealed sample was 0.66 K and it became 0.76 K upon Therm-ox, as shown in Fig. 1(b). This latter  $T_C$  value is close to that of the 4.7 nm thick PtSi film in the as-annealed sample (0.8 K). The observed increase in  $T_C$  due to Therm-ox, despite agglomeration leading to the threefold increase in  $RT R_s$ , can be attributed to the thickened [Fig. 2(f)] yet still electrically connected PtSi regions [Fig. 2(c)]. The grain size estimation also indicates enlarged PtSi grains to about 6 nm in the oxidized sample from around 3 nm in the as-annealed precursor [Fig. 2(a)]. Mass conserved, the agglomerated PtSi would indeed be about twice as thick for its 50% surface coverage [Fig. 2(c)]. Clearly,  $T_C$  is governed by the performance of the best percolating path in a superconducting film, whereas ordinary  $RT R_s$  is sensitive to the homogeneity of the conducting film itself.

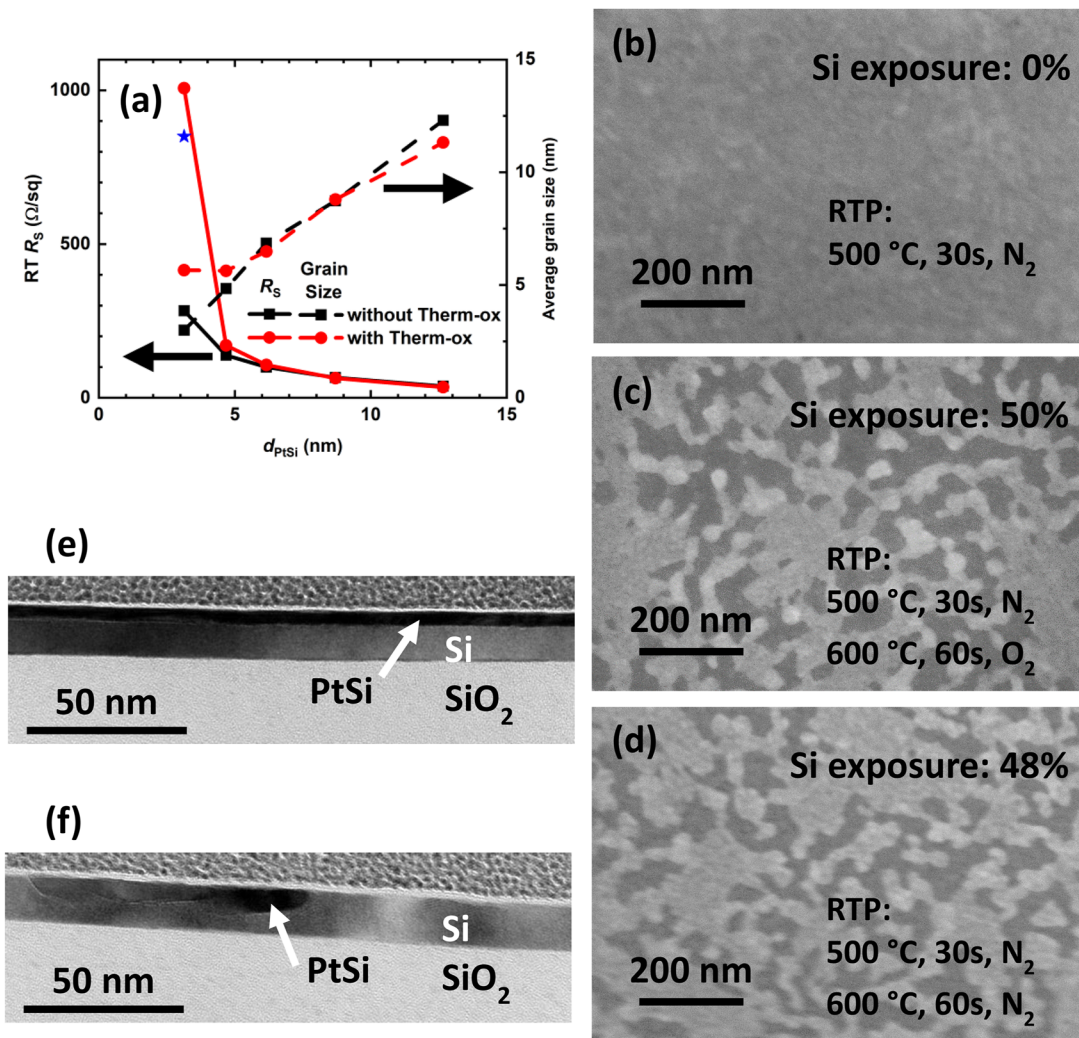


**FIG. 2.** (a)  $RT R_s$  and average grain size as a function of  $d_{\text{PtSi}}$  for PtSi films formed at 500 °C with or without surface thermal oxidation at 600 °C. The blue star represents the  $RT R_s$  of a 3.1 nm PtSi sample after sequential RTP in N<sub>2</sub> at 500 °C for 30 s and 600 °C for 60 s. Plan-view in-lens secondary electron SEM images for a 3.1 nm PtSi sample (b) after RTP at 500 °C, (c) after RTP at 500 °C and then surface thermal oxidation, and (d) after RTP in N<sub>2</sub> at 500 °C for 30 s and then 600 °C for 60 s. The bright parts are PtSi, while the dark parts are exposed Si. Cross-sectional TEM, XTEM, images for (e) the sample in (b) showing the formation of an ultrathin and uniform PtSi layer and (f) the sample in (c) showing a PtSi island embedded in Si. Pt was deposited on the sample surface for XTEM sample preparation.

The adverse thermal effect leading to the agglomeration of ultrathin PtSi films can be circumvented by replacing Therm-ox in oxygen at 600 °C with Chem-ox in piranha below 100 °C. The quality of the chemically grown oxide for PtSi protection against attack by aqua regia is evaluated using two sets of PtSi films formed at 500 °C and then separately oxidized with two recipes, either H<sub>2</sub>SO<sub>4</sub>:H<sub>2</sub>O<sub>2</sub> = 3:1 at RT for 5 min (Chem-ox-1) or H<sub>2</sub>SO<sub>4</sub>:H<sub>2</sub>O<sub>2</sub> = 4:1 at 80 °C for 30 min (Chem-ox-2). Selective etch in aqua regia was then applied to both samples. The  $RT R_s$  of the samples remained unaltered after Chem-ox and selective etch, indicating that the PtSi films were well protected against the etch, as shown by the continuous surface in Fig. 3(a). A well-layered structure with a

uniform 3.1 nm thick PtSi and a homogeneous surface SiO<sub>x</sub> desired for the SALICIDE process are shown in Fig. 3(b) by imaging and Fig. 3(c) by composition. In addition, after applying the aqua regia etch neither the  $RT R_s$  measurement nor the surface inspection done by means of SEM showed appreciable difference between the two Chem-ox samples. Furthermore, the  $RT R_s$  only slightly increased by <1% after either Chem-ox recipe, and no other phase than PtSi was detected by means of GIXRD within the sensitivity limit. Consequently,  $T_C$  of the PtSi films did not change after Chem-ox. An additional annealing step at 400–500 °C could be applied to convert the surface PtSi<sub>x</sub> ( $x < 1$ , likely formed due to preferential oxidation of the Si in PtSi<sup>21</sup>) back to PtSi. Thus, the piranha-based surface chem-

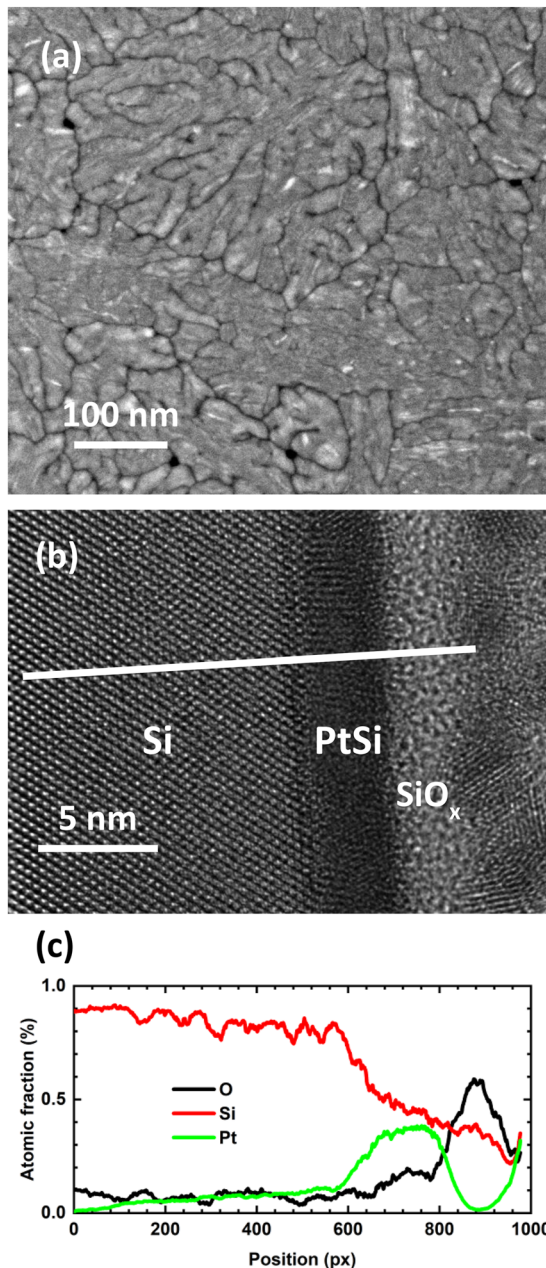


**FIG. 3.** (a) Plan-view high-angle annular dark field (HAADF) TEM image, (b) XTEM image, and (c) line-scan across the interface region, marked by the white line in (b), for composition analysis by means of EDS, for the 3.1 nm PtSi sample after RTP at 500 °C and then surface chemical oxidation (Chem-ox). The surface Pt peak comes from the deposited Pt for XTEM sample preparation.

ical oxide on the PtSi films, possibly grown self-limitedly, is shown to be effective in protecting the formed PtSi.

To conclude, this work demonstrates a simple and robust SALICIDE process for the formation of superconducting PtSi films below 5 nm in thickness. By replacing the thermal oxidation with

a chemical process, film agglomeration can be prevented. Low-temperature properties of the ultrathin PtSi films can be correlated with their structural variations and are investigated for their potential in quantum computing based on the Si-based JoFET.

We thank Robert Frost and Petter Ström at the Tandem Laboratory, Uppsala University, for RBS data acquisition. This project was partially funded within the QuantERA II Program that has received funding from the European Union's Horizon 2020 research and innovation program under Grant Agreement No 101017733. Additional funding was provided by the Swedish Research Council (2021–06025), the European project MATQu (Grant No. 101007322), the French National Research Agency (SUNISIDEuP – ANR-19-CE47-0010), the Grenoble LaBEX LANEF, and the Hungarian National Research, Development and Innovation Office (2019-2.1.7-ERA-NET-2022-00032). We acknowledge Myfab Uppsala for providing facilities and experimental support, with the support of Myfab as a national research infrastructure by the Swedish Research Council (2019-00207). We further acknowledge the infrastructural grants provided by the Swedish Research Council (VR-RFI No. 2017-00646\_9) and the Swedish Foundation for Strategic Research (SSF RIF14-0053) for supporting the accelerator operation. The microscopy facility was provided by the project VEKOP-2.3.3-15-2016-00002 of the European Structural and Investment Funds.

## AUTHOR DECLARATIONS

### Conflict of Interest

The authors have no conflicts to disclose.

### Author Contributions

**Yao Yao:** Data curation (equal); Formal analysis (equal); Investigation (equal); Methodology (equal); Visualization (equal); Writing – original draft (equal); Writing – review & editing (equal). **Daniel F. Fernandes:** Data curation (equal); Formal analysis (equal); Investigation (equal); Visualization (equal); Writing – review & editing (equal). **Tereza Košutová:** Data curation (equal); Formal analysis (equal); Investigation (equal); Visualization (equal); Writing – review & editing (equal). **Tomas Kubart:** Formal analysis (equal); Writing – review & editing (equal). **Zhen Zhang:** Formal analysis (equal); Funding acquisition (equal); Writing – review & editing (equal). **François Lefloch:** Data curation (equal); Formal analysis (equal); Funding acquisition (equal); Investigation (equal); Visualization (equal); Writing – review & editing (equal). **Frédéric Gustavo:** Data curation (equal); Investigation (equal); Visualization (equal); Writing – review & editing (equal). **Axel Leblanc:** Data curation (equal); Investigation (equal); Visualization (equal); Writing – review & editing (equal). **János L. Lábár:** Data curation (equal); Funding acquisition (equal); Investigation (equal); Visualization (equal); Writing – review & editing (equal). **Béla Pécz:** Funding acquisition (equal); Investigation (equal); Writing – review & editing (equal). **Shi-Li Zhang:** Conceptualization (lead); Formal analysis (equal); Funding acquisition (equal); Methodology (equal); Supervision (lead); Writing – original draft (equal); Writing – review & editing (equal).

## DATA AVAILABILITY

The data that support the findings of this study are available from the corresponding author upon reasonable request.

## REFERENCES

- <sup>1</sup>N. P. de Leon, K. M. Itoh, D. Kim, K. K. Mehta, T. E. Northup, H. Paik, B. S. Palmer, N. Samarth, S. Sangtawesin, and D. W. Steuerman, "Materials challenges and opportunities for quantum computing hardware," *Science* **372**(6539), eabb2823 (2021).
- <sup>2</sup>C. Outeiral, M. Strahm, J. Shi, G. M. Morris, S. C. Benjamin, and C. M. Deane, "The prospects of quantum computing in computational molecular biology," *Wiley Interdiscip. Rev.: Comput. Mol. Sci.* **11**(1), e1481 (2021).
- <sup>3</sup>A. Chatterjee, P. Stevenson, S. De Franceschi, A. Morello, N. P. de Leon, and F. Kuemmeth, "Semiconductor qubits in practice," *Nat. Rev. Phys.* **3**(3), 157–177 (2021).
- <sup>4</sup>S.-L. Zhang and Z. Zhang, "6—Metal silicides in advanced complementary metal-oxide-semiconductor (CMOS) technology," in *Met. Films Electron. Opt. Magn. Appl.*, edited by K. Barmak and K. Coffey (Woodhead Publishing, 2014), pp. 244–301.
- <sup>5</sup>T. I. Baturina, D. W. Horsell, D. R. Islamov, I. V. Drebuschak, Y. A. Tsaplin, A. A. Babenko, Z. D. Kvon, A. K. Savchenko, and A. E. Plotnikov, "Josephson junction arrays on the basis of superconducting PtSi films," *Physica B* **329–333**, 1496–1497 (2003).
- <sup>6</sup>M. J. Prest, J. S. Richardson-Bullock, Q. T. Zhao, J. T. Muhonen, D. Gunnarsson, M. Prunnila, V. A. Shah, T. E. Whall, E. H. C. Parker, and D. R. Leadley, "Superconducting platinum silicide for electron cooling in silicon," *Solid-State Electron.* **103**, 15–18 (2015).
- <sup>7</sup>P. Szypryt, B. A. Mazin, G. Ulbricht, B. Bumble, S. R. Meeker, C. Bockstiegel, and A. B. Walter, "High quality factor platinum silicide microwave kinetic inductance detectors," *Appl. Phys. Lett.* **109**(15), 151102 (2016).
- <sup>8</sup>M. Schwarz, T. D. Vethaak, V. Derycke, A. Francheteau, B. Iniguez, S. Kataria, A. Kloes, F. Lefloch, M. Lemme, J. P. Snyder, W. M. Weber, and L. E. Calvet, "The Schottky barrier transistor in emerging electronic devices," *Nanotechnology* **34**(35), 352002 (2023).
- <sup>9</sup>H. Riel, "Quantum computing technology," in *2021 IEEE International Electron Devices Meet. IEDM (IEEE, 2021)*, pp. 1.3.1–1.3.7.
- <sup>10</sup>M. Östling and C. Zaring, "Basic physical properties," in *Prop. Met. Silicides*, edited by K. Maex and M. van Rossum (INSPEC, 1995), pp. 1–52.
- <sup>11</sup>A. A. Naem, "Platinum silicide formation using rapid thermal processing," *J. Appl. Phys.* **64**(8), 4161–4167 (1988).
- <sup>12</sup>K. Oto, S. Takaoka, K. Murase, and S. Ishida, "Superconductivity in PtSi ultrathin films," *J. Appl. Phys.* **76**(9), 5339–5342 (1994).
- <sup>13</sup>D.-X. Xu, J. P. McCaffrey, S. R. Das, G. C. Aers, and L. E. Erickson, "Electrical and structural properties of PtSi films in deep submicron lines," *Appl. Phys. Lett.* **68**(25), 3588–3590 (1996).
- <sup>14</sup>R. A. Donaton, S. Jin, H. Bender, T. Conard, I. D. Wolf, K. Maex, A. Van-tomme, and G. Langouche, "New technique for forming continuous, smooth, and uniform ultrathin (3 nm) PtSi layers," *Electrochem. Solid-State Lett.* **2**(4), 195 (1999).
- <sup>15</sup>Z. D. Kvon, T. I. Baturina, R. A. Donaton, M. R. Baklanov, M. N. Kostrikin, K. Maex, E. B. Olshanetsky, and J. C. Portal, "Maki–Thompson corrections in thin superconducting PtSi films nearby  $T_c$ ," *Physica B* **284–288**, 959–960 (2000).
- <sup>16</sup>H. Bentmann, A. A. Demkov, R. Gregory, and S. Zollner, "Electronic, optical, and surface properties of PtSi thin films," *Phys. Rev. B* **78**(20), 205302 (2008).
- <sup>17</sup>R. A. Donaton, S. Jin, H. Bender, M. Zagrebnov, K. Baert, K. Maex, A. Van-tomme, and G. Langouche, "Formation of ultra-thin PtSi layers with a 2-step silicidation process," *Microelectron. Eng.* **37–38**, 507–514 (1997).
- <sup>18</sup>C. Kumpf, R. Nicula, and E. Burkel, "Growth and structure of thin Pt<sub>2</sub>Si and PtSi layers on Si(111) and (001) characterized with *in situ* grazing incidence diffraction," *J. Appl. Crystallogr.* **30**(6), 1016–1021 (1997).
- <sup>19</sup>S. R. Das, K. Sheergar, D.-X. Xu, and A. Naem, "Thickness dependence of the properties and thermal stability of PtSi films," *Thin Solid Films* **253**(1–2), 467–472 (1994).
- <sup>20</sup>T. Vethaak, "Silicide-based Josephson field effect transistors for superconducting qubits," Ph.D. thesis, Université Grenoble Alpes, 2021.
- <sup>21</sup>Z. Zhang, S.-L. Zhang, M. Östling, and J. Lu, "Robust, scalable self-aligned platinum silicide process," *Appl. Phys. Lett.* **88**(14), 142114 (2006).
- <sup>22</sup>C. Chang, "Formation of Pt silicides: The effect of oxygen," *J. Appl. Phys.* **58**(3), 1412–1414 (1985).
- <sup>23</sup>E. F. Fabrizio, T. M. McEvoy, P. Jassel, J. Lozano, K. J. Stevenson, and A. J. Bard, "Electrochemical and surface characterization of platinum silicide electrodes and their use as stable platforms for electrogenerated chemiluminescence assays," *J. Electroanal. Chem.* **554–555**, 99–111 (2003).
- <sup>24</sup>U. Holzwarth and N. Gibson, "The Scherrer equation versus the 'Debye-Scherrer equation,'" *Nat. Nanotechnol.* **6**(9), 534 (2011).
- <sup>25</sup>Z. Matěj, R. Kužel, and L. Nichtová, "XRD total pattern fitting applied to study of microstructure of TiO<sub>2</sub> films," *Powder Diffr.* **25**(2), 125–131 (2010).
- <sup>26</sup>J. Simonin, "Surface term in the superconductive Ginzburg–Landau free energy: Application to thin films," *Phys. Rev. B* **33**(11), 7830–7832 (1986).
- <sup>27</sup>A. M. Finkel'stein, "Suppression of superconductivity in homogeneously disordered systems," *Physica B* **197**(1–4), 636–648 (1994).
- <sup>28</sup>Y. Ivry, C.-S. Kim, A. E. Dane, D. De Fazio, A. N. McCaughan, K. A. Sunter, Q. Zhao, and K. K. Berggren, "Universal scaling of the critical temperature for thin films near the superconducting-to-insulating transition," *Phys. Rev. B* **90**(21), 214515 (2014).
- <sup>29</sup>T. D. Vethaak, F. Gustavo, T. Farjot, T. Kubart, P. Gergaud, S.-L. Zhang, F. Nemouchi, and F. Lefloch, "Influence of substrate-induced thermal stress on the superconducting properties of V<sub>3</sub>Si thin films," *J. Appl. Phys.* **129**(10), 105104 (2021).
- <sup>30</sup>P. Gas and F. M. d'Heurle, "Kinetics of formation of TM silicide thin films: Self-diffusion," in *Prop. Met. Silicides*, edited by K. Maex and M. van Rossum (INSPEC, 1995), p. 284.